RESEARCH ARTICLE

Scleraxis and osterix antagonistically regulate tensile force-responsive remodeling of the periodontal ligament and alveolar bone

Aki Takimoto[1,*], Masayoshi Kawatsu[1,2,*], Yuki Yoshimoto[3], Tadafumi Kawamoto[4], Masahiro Seiryu[2], Teruko Takano-Yamamoto[2], Yuji Hiraki[1] and Chisa Shukunami[1,3,‡]

ABSTRACT

The periodontal ligament (PDL) is a mechanosensitive noncalcified fibrous tissue connecting the cementum of the tooth and the alveolar bone. Here, we report that scleraxis (Scx) and osterix (Osx) antagonistically regulate tensile force-responsive PDL fibrogenesis and osteogenesis. In the developing PDL, Scx was induced during tooth eruption and co-expressed with Osx. Scx was highly expressed in elongated fibroblastic cells aligned along collagen fibers, whereas Osx was highly expressed in the perialveolar/apical osteogenic cells. In an experimental model of tooth movement, Scx and Osx expression was significantly upregulated in parallel with the activation of bone morphogenetic protein (BMP) signaling on the tension side, in which bone formation compensates for the widened PDL space away from the bone under tensile force by tooth movement. Scx was strongly expressed in Scx^+/Osx^+ and Scx^+/Osx^- fibroblastic cells of the PDL that does not calcify; however, Scx^-/Osx^+ osteogenic cells were dominant in the perialveolar osteogenic region. Upon BMP6-driven osteoinduction, osteocalcin, a marker for bone formation was downregulated and upregulated by *Scx* overexpression and knockdown of endogenous *Scx* in PDL cells, respectively. In addition, mineralization by osteoinduction was significantly inhibited by *Scx* overexpression in PDL cells without affecting *Osx* upregulation, suggesting that Scx counteracts the osteogenic activity regulated by Osx in the PDL. Thus, Scx^+/Osx^-, Scx^+/Osx^+ and Scx^-/Osx^+ cell populations participate in the regulation of tensile force-induced remodeling of periodontal tissues in a position-specific manner.

KEY WORDS: Scleraxis, Osterix, Periodontal ligament, Tensile force, Mouse

INTRODUCTION

The periodontal ligament (PDL) is a multifunctional fibrous tissue that physically connects the cementum covering the tooth root to the cortical surface of the alveolar bone (Beertsen et al., 1997). Despite its osteogenic potential, as evidenced by its high level of alkaline phosphatase (ALP) activity (Yamashita et al., 1987), the PDL

between the cementum and the alveolar bone is fibrous and maintains its width unmineralized under both physiological and orthodontic conditions (Beertsen et al., 1997). The PDL senses multidirectional mechanical forces, such as mastication, speech and orthodontic tooth movement (Mabuchi et al., 2002; Pavlin and Gluhak-Heinrich, 2001). Under physiological conditions, the position of teeth in their sockets is maintained by establishing a dynamic equilibrium between bone resorption and apposition at the PDL-bone interface exposed to a variety of mechanical stimuli (Pavlin and Gluhak-Heinrich, 2001; Takano-Yamamoto et al., 1994). On application of orthodontic force, proliferation of osteogenic cells and mineralization of the extracellular matrix (ECM) occur on the tension side, whereas the compressed region within the PDL shows increased osteoclastic activity (Beertsen et al., 1997; Terai et al., 1999). Hence, the PDL is a mechanoresponsive tissue that is essential for not only the maintenance of its space and the tooth socket but also tooth movement.

The PDL contains a variety of cell populations, consisting of fibroblasts, osteoblasts, osteoclasts, cementoblasts, endothelial cells, sensory cells and progenitor/stem cells (Beertsen et al., 1997; Seo et al., 2004), thus enabling the PDL to perform supportive, remodeling, sensory, nutritive and homeostatic functions. It appears that a certain population of PDL cells is tensile force-responsive and has the unique ability to switch cellular differentiation state into either fibroblastic or osteogenic, depending on the position of the cells in the PDL. However, it remains unclear how PDL cells regulate the balance between fibrogenesis and osteogenesis by transducing mechanical force into the biological mediators.

Osteogenic differentiation is regulated by runt-related transcription factor 2 (Runx2) and osterix (Osx; Sp7 – Mouse Genome Informatics) (Komori et al., 1997; Nakashima et al., 2002). Osx is a zinc-finger-containing transcription factor that regulates the differentiation of pre-osteoblasts into fully functional osteoblasts and cementoblasts (Cao et al., 2012; Nakashima et al., 2002). Unlike bone formation, the molecular mechanisms governing ligament formation are not fully understood. Scleraxis (Scx) is a basic helix-loop-helix transcription factor that is predominantly expressed in the tendon/ligament cell lineage (Brent et al., 2003; Cserjesi et al., 1995; Schweitzer et al., 2001; Sugimoto et al., 2013a, b). *Scx* is reportedly required for the formation and maturation of force-transmitting and intermuscular tendons (Murchison et al., 2007). The expression of the type I collagen and tenomodulin (*Tnmd*) in tenocytes is positively regulated by *Scx* (Murchison et al., 2007; Shukunami et al., 2006). Cellular adhesion in the PDL is enhanced by *Tnmd* overexpression and decreased by a loss of *Tnmd* (Komiyama et al., 2013). Mechanical forces also modulate the expression of *Scx* in tendons *in vivo* and *in vitro* (Maeda et al., 2011; Scott et al., 2011).

[1]Department of Cellular Differentiation, Institute for Frontier Medical Sciences, Kyoto University, Kyoto 606-8507, Japan. [2]Department of Orthodontic and Dentofacial Orthopedics, Tohoku University Graduate School of Dentistry, Sendai 980-8575, Japan. [3]Department of Molecular Biology and Biochemistry, Division of Basic Life Sciences, Institute of Biomedical & Health Sciences, Hiroshima University, Hiroshima 734-8553, Japan. [4]Radioisotope Research Institute, Tsurumi University School of Dental Medicine, Tsurumi, Yokohama 230-8501, Japan.
*These authors contributed equally to this work

‡Author for correspondence (shukunam@hiroshima-u.ac.jp)

DEVELOPMENT

In our present study, taking advantage of *ScxGFP*-transgenic (Tg) mice that express enhanced green fluorescent protein (GFP) under the control of the promoter/enhancer of the mouse *Scx* gene (Sugimoto et al., 2013b), we demonstrated that Scx and Osx are significantly upregulated on the tension side in parallel with the activation of bone morphogenetic protein (BMP) signaling. Scx is strongly expressed in Scx^+/Osx^+ and Scx^+/Osx^- cells that are localized to the unmineralized middle zone of the PDL. By contrast, Osx is highly expressed in Scx^-/Osx^+ PDL cells in the perialveolar zone, in which new bone formation takes place. Under osteoinductive culture conditions, lentiviral overexpression of *Scx* in PDL cells inhibited mineralization without affecting *Osx* mRNA levels. Thus, the counteracting effect of Scx on Osx-driven osteogenesis regulates tensile force-responsive PDL remodeling, in which the fine balance of Scx^+/Osx^-, Scx^+/Osx^+ and Scx^-/Osx^+ cell populations contributes to the maintenance of the physiological junctional attachments between teeth and bones in a position-specific manner in response to mechanical stress.

RESULTS

Induction of *Scx* expression in the PDL and the odontoblast-predentin layer during tooth eruption

We analyzed Scx expression in dental tissue (Fig. 1A) using *ScxGFP* Tg mice, which express GFP in the tendon and ligament cell lineages. To visualize calcified tissues, the frozen sections were immunostained with osteocalcin (Ocn; Bglap – Mouse Genome Informatics), which is detected in tooth and periodontal tissues (Takano-Yamamoto et al., 1994). In 2-, 3- and 4-week-old *ScxGFP* Tg mice, alveolar bone and dentin were immunostained intensely with the anti-Ocn antibody (Fig. 1B-E). In an unerupted maxillary second molar of a 2-week-old *ScxGFP* Tg mouse, only PDL cells in the distal region of the root expressed Scx at low levels, as

monitored by GFP expression (arrows in Fig. 1B,C). At the third postnatal week, Scx became detectable throughout the PDL, except for the periapical region, during eruption of molar teeth (Fig. 1D). In a second molar of a 4-week-old *ScxGFP* Tg mouse, Scx was detected in the PDL and odontoblast-predentin layer (arrowheads in Fig. 1E). These results are consistent with endogenous *Scx* expression detected by *in situ* hybridization (supplementary material Fig. S1).

For a more detailed analysis, we compared the expression of periostin (Pstn; Postn – Mouse Genome Informatics), a major ECM component of the PDL (Ma et al., 2011), with the expression of Scx. In a maxillary second molar of a 6-week-old *ScxGFP* Tg mouse, Pstn was localized to the gingival lamina propria (red arrowheads in Fig. 1F), PDL and Sharpey's fibers entering the alveolar bone and cementum (Fig. 1F). Scx was detected in the Pstn-positive PDL (Fig. 1F,G). Interestingly, PDL cells expressed Scx at varied levels depending on their position within the PDL. Weak Scx expression was observed in the periapical PDL (arrows in Fig. 1F,G), whereas Scx was highly expressed in the cervical PDL (asterisks in Fig. 1F,G). PDL cells expressing Scx at a higher level exhibited a more flattened and elongated morphology in the cervical region (Fig. 1J,K). These results suggest that the stress-strain levels within the PDL in response to physiological mechanical forces affect Scx expression in PDL cells.

Characterization of PDL cells

Tenocytes and ligamentocytes express *Scx* and *Tnmd* similarly (Sugimoto et al., 2013a). We compared the marker gene expression of PDL cells with that of tenocytes isolated from limb tendons (supplementary material Fig. S2). *Scx* and *Pstn* were expressed in PDL cells and tenocytes at similar levels. Both tenascin C (*Tnc*) and type I collagen (*Col1a1*) were expressed in tenocytes, but *Tnc* was
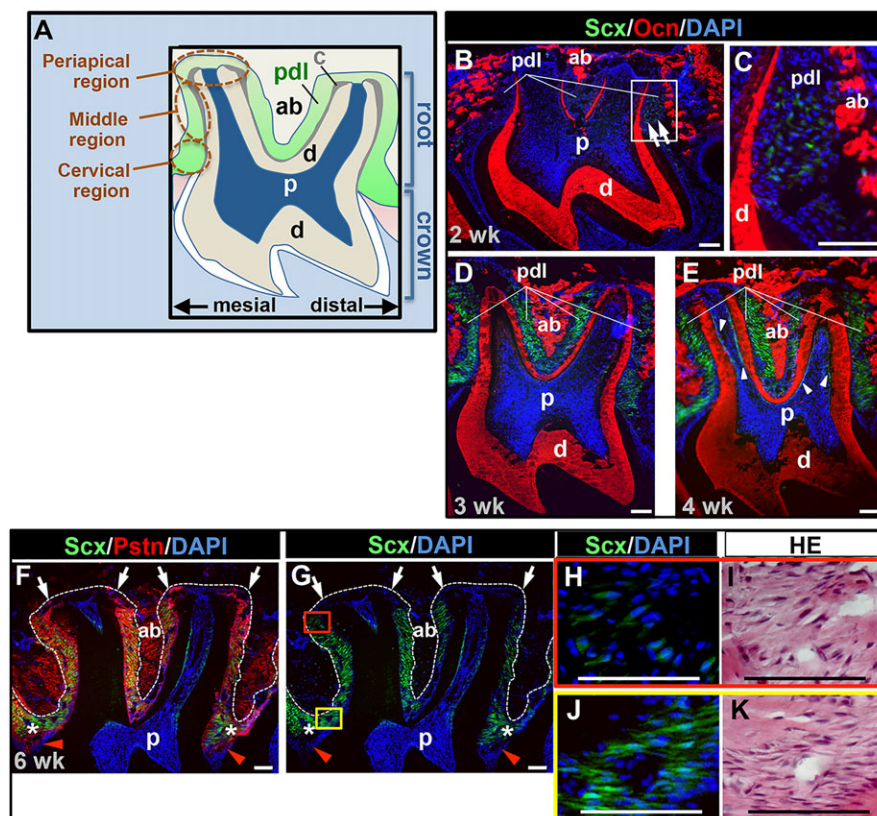

Fig. 1. Expression of Scx during tooth root formation. (A) Schematic of a mouse maxillary second molar with periodontal tissues. (B-K) Undecalcified frozen sections from the maxillary second molars of 2- (B,C), 3- (D), 4- (E) and 6-week-old (F-K) *ScxGFP* Tg mice were processed for immunostaining of GFP (green) and Ocn (red) or Pstn (red). The nuclei were stained with DAPI (blue). The sections shown in F-H,J were stained with HE (I,K) after the acquisition of fluorescent images. The boxed region in B is shown at a higher magnification in C. Arrows in B indicate the region that is positive for faint Scx signals in the PDL of a 2-week-old *ScxGFP* Tg mouse. White arrowheads in E indicate Scx expression in odontoblasts of a 4-week-old *ScxGFP* Tg mouse. Arrows and asterisks in F,G indicate the periapical and cervical regions of the PDL, respectively. Red arrowheads in F,G indicate the Scx-negative tissue of the gingival lamina propria in which Pstn is localized. The boundaries between the PDL and alveolar bone are shown by dashed lines (F,G). The red and yellow boxed regions in G are shown at higher magnification in H,I and in J,K, respectively. ab, alveolar bone; c, cementum; d, dentin; p, pulp; pdl, periodontal ligament. Scale bars: 100 μm.
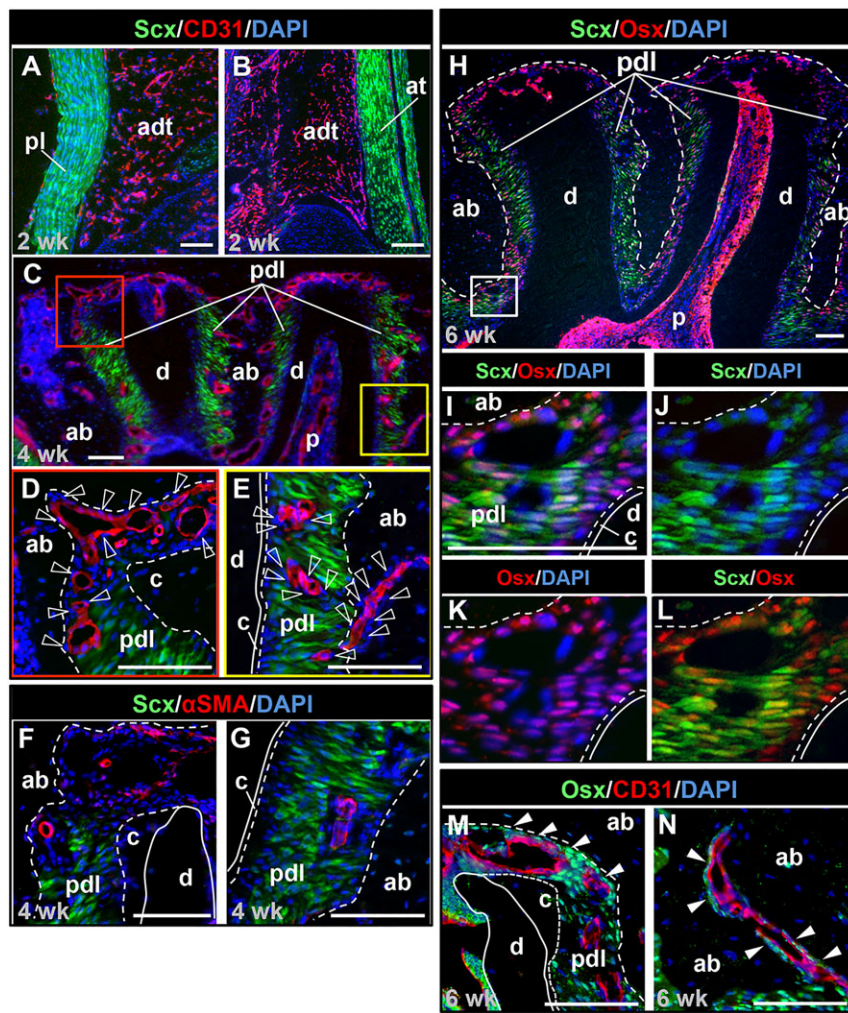
Fig. 2. Expression of Scx, Osx, αSMA and CD31 in the PDL of developing periodontal tissues. (A-N) Undecalcified frozen sections from the leg of a 2-week-old *ScxGFP* Tg mouse (A,B) and the maxillary second molars of 4- (C-G) or 6-week-old (H-L) *ScxGFP* Tg mice were processed for immunostaining of GFP (green) and CD31 (red) (A-E), αSMA (red) (F,G) or Osx (red) (H-L). The maxillary second molar of a 6-week-old wild-type mouse was processed for immunostaining of Osx (green) and CD31 (red) (M,N). The nuclei were stained with DAPI (blue). Scx expression was monitored by GFP expression (A-J,L). CD31$^+$ endothelial cells were not observed in the patella ligament (A) or Achilles tendon (B), but were present in the PDL (C). The red and yellow boxed regions in C are shown at higher magnification in D and in E, respectively. The periapical and middle regions of the PDL are shown in F and in G, respectively. The white boxed region in H is shown at higher magnification in I-L. Empty arrowheads in D,E indicate Scx$^-$ cells localized in perivascular regions. White arrowheads in M, N indicate Osx$^+$ cells localized in close proximity to endothelial cells. Lines in E,F,G,I-M indicate the boundaries between the cementum and the dentin. Dashed lines in D-M indicate the boundaries between the PDL and cementum or alveolar bone. ab, alveolar bone; adt, adipose tissue; at, Achilles tendon; c, cementum; d, dentin; p, pulp; pdl, periodontal ligament; pl, patella ligament. Scale bars: 100 µm.

undetectable in PDL cells. The expression of *Col1a1* was higher in PDL cells than in tenocytes. *Osx* was expressed in PDL cells, but its expression was undetectable in tenocytes.

Tendons and ligaments are hypovascular dense connective tissue that is made up of regular bundles of collagen fibers, whereas bone, especially in newly forming areas, is highly vascularized (Benjamin and Ralphs, 2000; Docheva et al., 2005; Maes et al., 2010; Shukunami et al., 2008). CD31$^+$ vascular endothelial cells were observed scarcely in the patella ligament (Fig. 2A) and Achilles tendon (Fig. 2B). By contrast, the PDL was penetrated by blood vessels (Fig. 2C), suggesting that the PDL is distinct from ligament binding to adjacent bones in terms of its anti-angiogenic property. It has been suggested that progenitor cells expressing alpha-smooth muscle actin (αSMA) reside in the perivascular regions of the PDL and differentiate into osteoblasts, cementoblasts and fibroblasts (Roguljic et al., 2013; San Miguel et al., 2010). Consistent with previous findings, Scx$^+$ cells were not localized in close proximity to the perivascular regions (empty arrowheads in Fig. 2D,E). The expression of αSMA in perivascular cells in the PDL did not overlap with the expression of Scx (Fig. 2F,G). This suggests that Scx-expressing PDL cells are comparatively mature fibroblastic cells that maintain the ligamentous tissue of erupted teeth. Osx was detectable throughout the PDL as well as the pulp (Fig. 2H). At this stage, almost all Scx$^+$ PDL cells were positive for Osx (Fig. 2H-L). Osx was also expressed at a higher level in Scx$^-$ perivascular cells in the periapical PDL and alveolar bone (white arrowheads in Fig. 2M,N).

To investigate the characteristics of Scx$^+$ cell populations in the PDL after tooth root formation is completed, we analyzed ALP activity and Osx expression in a 12-week-old *ScxGFP* Tg mouse (Fig. 3). In the leg (Fig. 3A), ALP activity was detectable in cartilaginous and bony tissues, but undetectable in Scx$^+$ tendons and ligaments (Fig. 3B). Osx was expressed in immature osteoblasts (arrowheads in Fig. 3C) and prehypertrophic/hypertrophic chondrocytes (data not shown), but was undetectable in Scx$^+$ cells in the tendons and ligaments of the leg (Fig. 3C,D). In a maxillary second molar of a 12-week-old *ScxGFP* Tg mouse, ALP activity was detected in cells throughout the PDL as well as in dental pulp cells (Fig. 3E). Osx was expressed in osteoblasts, cementoblasts, odontoblasts and PDL cells (Fig. 3F). In the periapical region, some Osx$^+$ cells were detected in the PDL that comprised cells with weak or no Scx expression (Fig. 3G,H). In the oblique fibers of the PDL, overlapping Scx and Osx expression was detected in a subset of fibroblastic cells (yellow arrowheads in Fig. 3I,J) that were neither perivascular nor osteoblastic/cementoblastic cells. These results indicate that Scx$^+$ PDL cells *in vivo* retain an osteogenic phenotype with high ALP activity and Osx expression, different from fibroblasts in tendons and ligaments.

Upregulation of Scx by tensile force during experimental tooth movement

Under physiological conditions, Scx was expressed at a high level in elongated PDL cells under tensile force as a result of stretching of the PDL by trans-septal fibers between the molars (Fig. 1). This
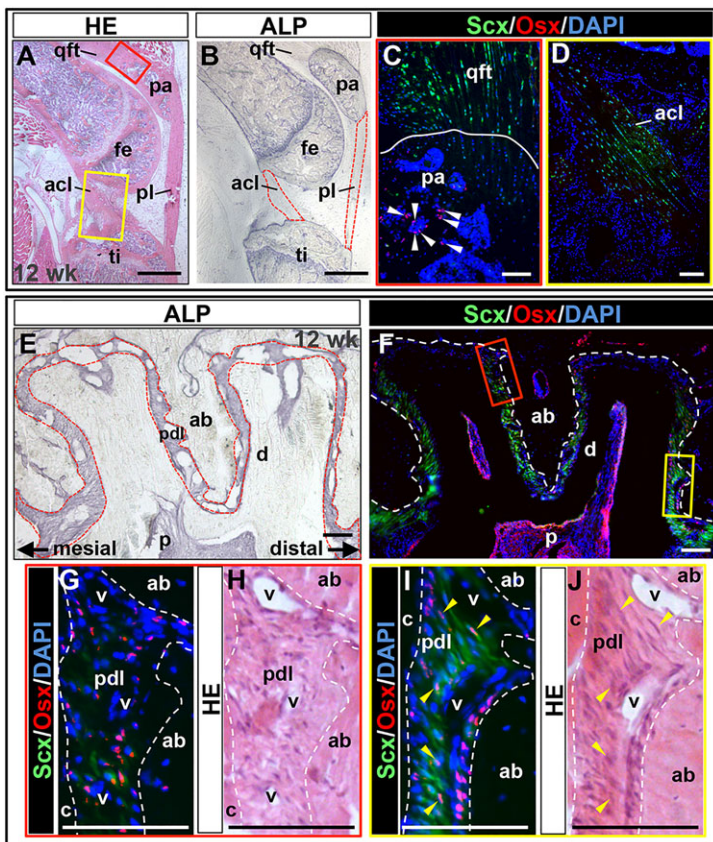
Fig. 3. ALP staining and Osx expression in the PDL.
(A-J) Undecalcified frozen sections from the leg (A-D) or the maxillary second molar (E-J) of a 12-week-old *ScxGFP* Tg mouse were processed for the detection of ALP activity or immunostaining of GFP (green) and Osx (red). The nuclei were stained with DAPI (blue) (C,D,F,G,I). The sections (C,D,F,G,I) were stained with HE (A,H,J) after the acquisition of fluorescent images. The red and yellow boxed regions in A correspond to the fluorescent images of C and of D, respectively. The boundary between the quadriceps femoris tendon and calcified region of the patella is shown by a white line (C). White arrowheads in C indicate Osx$^+$ osteoblasts in the patella. The red and yellow boxed regions in F correspond to the fluorescent and HE images of G,H and of I,J, respectively. The regions of ligamentous tissues in B,E are encircled by red dashed lines. The boundaries between the PDL and the alveolar bone (F,G-J) or the cementum (G-J) are shown by white dashed lines. Yellow arrowheads in I,J indicate Scx$^+$/Osx$^+$ fibroblasts. ab, alveolar bone; acl, anterior cruciate ligament; c, cementum; d, dentin; fe, femur; p, pulp; pa, patella; pdl, periodontal ligament; patella ligament; qft, quadriceps femoris tendon; ti, tibia; v, blood vessel. Scale bars: 1 mm in A,B; 100 µm in C-J.

observation raises the possibility that tensile force on the PDL positively regulates Scx expression. We then examined Scx expression during experimental tooth movement by monitoring GFP expression in *ScxGFP* Tg mice (Fig. 4A,B). At 48 h after the experimental tooth movement, the distance between the first and second molars increased by 107.8±15.4 µm (mean±s.d., *n*=4). In transverse sections of maxillary first molars with experimental tooth movement, Scx upregulation was observed clearly in the PDL on the tension sides (arrowheads in Fig. 4D) compared with the corresponding regions on the contralateral control side (Fig. 4C). By the insertion of an elastic band, widening of the PDL space and elongated fibroblastic cells were observed on the tension side (Fig. 4E,F). High levels of Scx expression were induced in PDL cells by tensile force exerted by experimental tooth movement (arrowheads in Fig. 4G,H). To quantify the increase in Scx expression, we calculated the proportion of cells expressing Scx at a high level (Scx^{high}) to the total pool of cells expressing Scx (*n*=4) (supplementary material Table S1). The mean proportion of Scx^{high} cells was significantly increased on the experimental side (48.7%) compared with the control side (27.5%) (Fig. 4I). In RT-qPCR analysis, significant upregulation of *Scx* was detected in periodontal tissues on the experimental side (1.26-fold, *P*=0.02) compared with the control side (supplementary material Fig. S3). Upregulation of *Pstn* expression was also detected in the tensioned regions of the experimental side (1.57-fold, *P*=0.01) (supplementary material Fig. S3). Because bone formation is facilitated on the tension side of alveolar bone, it has been proposed that the PDL on the tension side is exposed to more osteogenic factors than in its unloaded state (Henneman et al., 2008). Consistent with this notion, phosphorylation of Smad1/5 for the BMP pathway was significantly increased on the tension side (Fig. 5A-H). Osx$^+$ cells were also increased on the tension side (Fig. 5I-P). Upon tensile loading, the proportion of cells

positive for pSmad1/5 and Osx in Scx$^+$ PDL cells was increased 1.91- and 1.39-fold, respectively (Fig. 5Q). Furthermore, the number of Scx^{high}/Osx$^+$ PDL cells (white arrowheads in Fig. 5I,M) was also increased in response to tensile force (2.49-fold, Fig. 5Q). Thus, it can be concluded that both Scx and Osx are tensile force-responsive transcription factors.

Inhibitory action of *Scx* on mineralization of the ECM of PDL cells
To elucidate the role of Scx in the PDL in response to osteogenic stimuli, we performed lentiviral overexpression of *Scx* in PDL cells (Fig. 6A). Successful overexpression of *Scx* in *LV-Scx*-infected cells on day 10 was confirmed by GFP expression and RT-PCR (Fig. 6B-D). Mineral deposition was monitored in osteo-inducing cultures on day 25 (Fig. 6E). Notably, formation of the calcified nodules in PDL cells overexpressing *Scx* was significantly suppressed compared with that in *Lv-Vec*-infected cells (Fig. 6E). The expression of *Runx2*, *Osx*, *osteopontin* (*Opn*; *Spp1* – Mouse Genome Informatics) and *Ocn* was significantly increased in PDL cells in response to osteogenic stimuli (Fig. 6F,G). Although the expression levels of *Runx2* and *Osx* were not affected by *Scx* overexpression (Fig. 6F), *Opn* and *Ocn* expression was significantly downregulated by *Scx* overexpression under osteo-inducing conditions (Fig. 6G). Among the non-osteogenic genes examined here, endogenous *Scx*, *matrix Gla protein* (*Mgp*), *Pstn* and *Tnmd* were significantly upregulated by *Scx* overexpression under non-inducing conditions (supplementary material Fig. S4). Under osteo-inducing conditions, *Pstn* and *Tnmd* expression was significantly decreased compared with that under non-inducing conditions (gray bars in supplementary material Fig. S4), whereas the expression level of *Pstn* recovered to that observed in *Lv-Vec*-infected cells under the non-inducing conditions by *Scx* overexpression (black bar of *Pstn* in supplementary
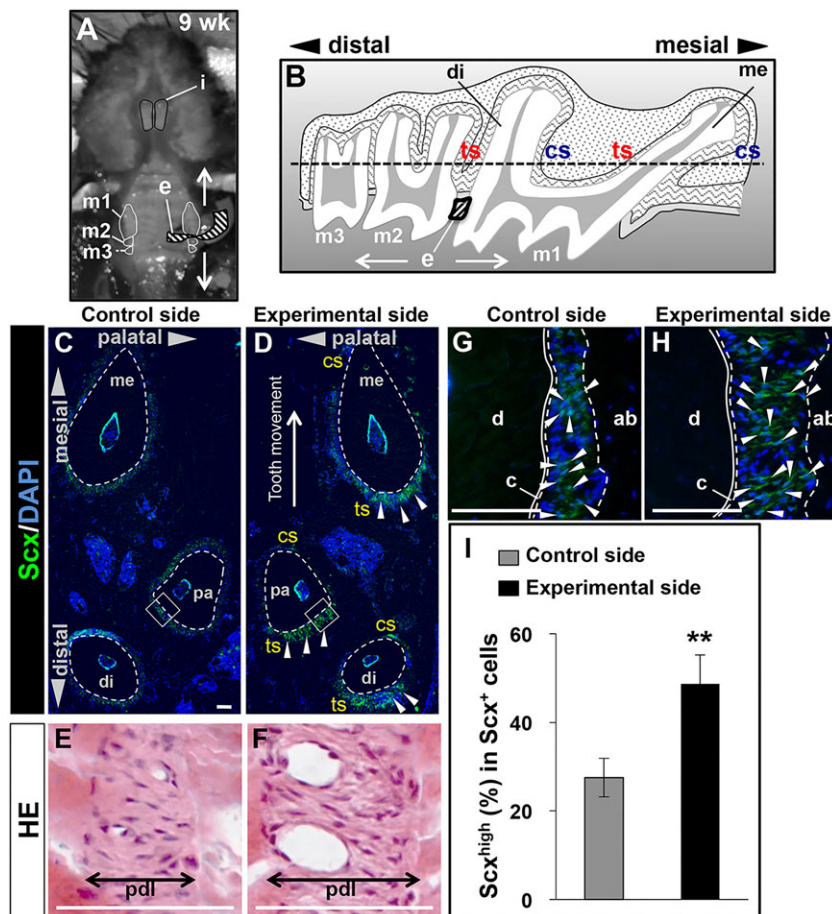
Fig. 4. Upregulation of Scx in PDL cells in response to tensile force exerted by experimental tooth movement.
(A) The upper jaw (view from palatal side) of a 9-week-old *ScxGFP* Tg mouse. The incisors and molars are enclosed by black and white lines, respectively. A piece of an elastic band was inserted interproximally between the upper left first and second molars. The right side served as control.
(B) Schematic of the sagittal plane of the maxillary molars with an inserted elastic band. The black dashed line indicates the sectioning level for the transverse sections shown in C-H. (C-H) Undecalcified frozen sections of the maxillary first molars (m1) of 9-week-old *ScxGFP* Tg mice were obtained at 48 h after insertion of an elastic band. The transverse sections were processed for immunostaining of GFP (green) (C,D,G,H). The nuclei were stained with DAPI (blue). The sections were stained with HE (E,F) after the acquisition of fluorescent images. White arrowheads in D indicate the tension side of the PDL expressing Scx at a high level. Images shown in E-H are the distal side of the PDL of the palatal root. The boxed regions in C and D correspond to the areas shown at higher magnification in G and in H, respectively. White arrows in B,D indicate the direction of tooth movement induced by the insertion of an elastic band. Black double arrows in E,F indicate the width of the PDL. White arrowheads in G,H indicate Scx^{high} cells in the PDL. The boundaries between the cementum and dentin are shown with lines (G,H). The boundaries between the PDL and alveolar bone (G,H) or cementum (C,D,G,H) are shown by white dashed lines. (I) Proportion of Scx^{high} cells to total Scx$^+$ cells in the corresponding regions of the boxed regions in C,D is shown. Values represent the mean±s.d. of the control and experimental sides (*n*=4). **$P<0.01$ versus control side. ab, alveolar bone; c, cementum; cs, compression side; d, dentin; di, distal root; e, elastic band; i, incisor; m, molar; me, mesial root; pa, palatal root; pdl, periodontal ligament; ts, tension side. Scale bars: 100 µm.

material Fig. S4). The level of *Mgp* in response to osteoinduction was further increased by *Scx* overexpression (gray and black bars in supplementary material Fig. S4). We then knocked down *Scx* by RNA interference (Fig. 7A). In PDL cells transfected with *siScx-1* or *siScx-2*, the level of *Scx* was decreased to less than 10% on day 6 (Fig. 7B). Although transient knockdown by siRNA did not significantly affect mineralization on day 6 (data not shown), gene silencing of *Scx* resulted in a marked increase of *Ocn* expression in PDL cells cultured under osteogenic conditions (Fig. 7C). No significant increase of *Ocn* expression by *Scx* siRNA was detected under non-inducing conditions (Fig. 7C). Taken together, these findings suggest that tensile force-responsive Scx has an inhibitory action on mineralization by regulating the expression of ECM molecules.

DISCUSSION
PDL cells have a unique differentiation potential in response to mechanical stimuli. In this study, we demonstrated that the Scx$^+$/Osx$^-$, Scx$^+$/Osx$^+$, Scx$^-$/Osx$^+$ PDL cell populations contribute coordinately to tensile force-induced remodeling of the PDL to maintain the junction between the cementum of the tooth and the alveolar bone. The *Scx* overexpression and knockdown experiments demonstrate that Scx negatively regulates the expression of osteogenic genes (*Opn* and *Ocn*) only under osteo-inducing conditions. The balance between fibrogenesis and osteogenesis in the tensile force-loaded PDL is regulated antagonistically by Scx and Osx in a position-specific manner (Fig. 8).

Scx is expressed predominantly in developing tendons and ligaments exposed to mechanical loading (Schweitzer et al., 2001; Sugimoto et al., 2013a). The gradual and temporary loss of tensile

loading results in the reversible loss of Scx expression in tendons (Maeda et al., 2011), whereas Scx expression is enhanced by cyclic loading *in vitro* (Scott et al., 2011). Our *in vivo* study using *ScxGFP* Tg mice revealed that Scx is induced in association with PDL maturation and is strongly expressed in elongated fibroblastic cells when they were exposed to tensile stress transmitted from collagen fibers running between the tooth and alveolar bone. During experimental tooth movement, Scx and Osx expression was significantly upregulated on the tension side, in which bone formation compensates for tooth movement away from the bone under tensile force. These results suggest that *Scx* is a tensile force-inducible gene in the PDL under physiological and orthodontic conditions.

We reported that Scx positively regulates the expression of *Tnmd*, which has anti-angiogenic activity in its C-terminal cysteine-rich domain (Kimura et al., 2008; Oshima et al., 2004). In contrast to ligaments responsible for bone-to-bone connections, the PDL, localized between the alveolar bone and the cementum of the tooth, is exceptionally well vascularized, reflecting the high metabolic turnover of cellular and extracellular constituents. However, our double-immunostaining study revealed that Scx and CD31 were expressed in a mutually exclusive way within the PDL. Scx^{high} PDL cells are found away from the apical region of the developing tooth root, in which active angiogenesis takes place. *Scx* overexpression resulted in the upregulation of *Tnmd* in PDL cells, suggesting that Scx enhances the mature ligamentocyte phenotype. As reported previously, cellular adhesion is enhanced by *Tnmd* overexpression and decreased by a loss of *Tnmd* in the PDL (Komiyama et al., 2013). In the PDL, the Scx$^+$ cell population represents a group of
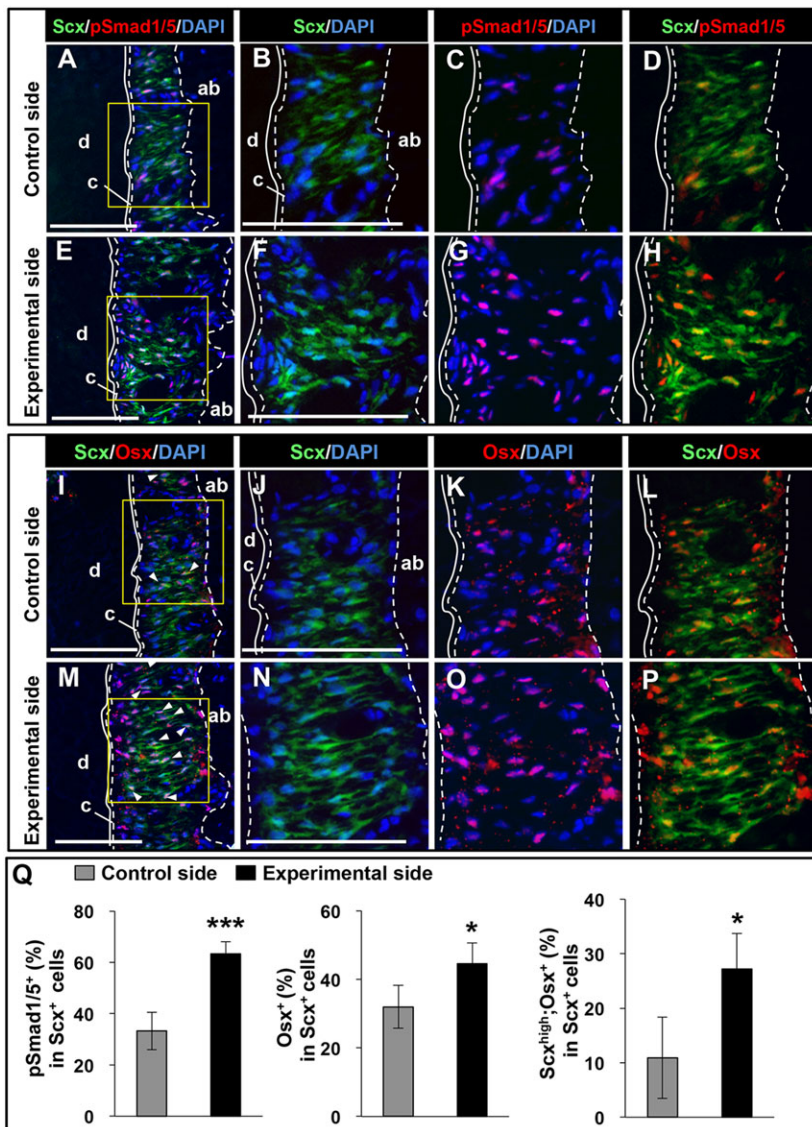
Fig. 5. Upregulation of pSmad1/5 and Osx in PDL cells in response to tensile force exerted by experimental tooth movement. (A-P) Undecalcified frozen sections of the maxillary first molars of 9-week-old *ScxGFP* Tg mice were obtained at 48 h after the start of experimental tooth movement. The transverse sections were processed for immunostaining of GFP (green) and pSmad1/5 (red) (A-H) or Osx (red) (I-P). The nuclei were stained with DAPI (blue). The regions of the control (A-D,I-L) and experimental (E-H,M-P) sides correspond to the boxed regions in Fig. 4C and D, respectively. The yellow boxed regions in A, E, I and M are shown at higher magnification in B-D, F-H, J-L and N-P, respectively. White arrowheads in I,M indicate cells expressing both Scx^{high} and Osx$^+$ (Scx^{high};Osx$^+$). The boundaries between the cementum and dentin are shown by white lines (A-M). The boundaries between the PDL and alveolar bone or cementum are shown by dashed lines (A-P). (Q) Proportion of pSmad1/5$^+$, Osx$^+$ or Scx^{high};Osx$^+$ cells to total Scx$^+$ cells is shown. Values represent mean±s.d. (*n*=4). *$P<0.05$ versus control side. ***$P<0.001$ versus control side. ab, alveolar bone; c, cementum; d, dentin. Scale bars: 100 μm.

mature ligamentocytes and its expression level varies, depending on the extent of tensile stress.

Osx is a zinc-finger-containing transcription factor that regulates the differentiation of pre-osteoblasts into fully functional osteoblasts (Nakashima et al., 2002). Genetic evidence suggests that Osx expression during tooth root formation is also closely associated with cementum formation (Cao et al., 2012). The number of Osx$^+$ cells in the PDL increase sharply in 4- to 6-week-old mice, whereas few Osx$^+$ cells are detected in the PDL of 6-month-old mice (Cao et al., 2012). Consistent with these findings, a number of Osx$^+$ cells were found in the developing PDL in 6-week-old mice, but Osx expression was decreased in the PDL of 12-week-old mice, the root formation of which is completed. In the experimental tooth movement model, Osx is upregulated in the PDL on the tension side undergoing bone formation. The Osx$^+$ cell population represents a group of cells committed to osteoblasts or cementoblasts in the PDL, thus contributing to the active remodeling of periodontal tissues.

Ectopic mineralization within ligaments causes tissue dysfunction. Ossification of the posterior longitudinal ligament of the spine causes spinal pain and, in severe cases, spinal cord compression (Inamasu et al., 2006). Despite the mechanical loading of mastication under physiological conditions or orthodontic forces during tooth movement, the PDL maintains its constant width unmineralized throughout the lifetime of an organism (Beertsen et al., 1997). Analysis of Scx-deficient mice revealed that Scx is essential for the condensation and differentiation of the progenitor cells for force-transmitting and intermuscular tendons, but no apparent morphological abnormality has been reported in developing ligaments (Murchison et al., 2007). However, we found a novel inhibitory action of Scx on mineralization by overexpression and knockdown experiments in PDL cells maintained under osteo-inducing conditions. *Scx* overexpression inhibited PDL mineralization without affecting *Runx2* or *Osx* mRNA levels, which were upregulated by osteoinduction. Conversely, the upregulated expression of *Ocn* by osteoinduction was increased further in PDL cells by gene silencing of *Scx*. Thus, in the osteogenic environment of the tensile force-loaded PDL, Scx might act as a negative regulator of alveolar bone formation to maintain the width of the PDL and to prevent ankylosis, that is, the fusion of the tooth root with the surrounding alveolar bone.

Molecules that negatively regulate mineralization are thought to play key roles in maintaining the homeostasis of the PDL trapped between the cementum and the alveolar bone. It has been reported
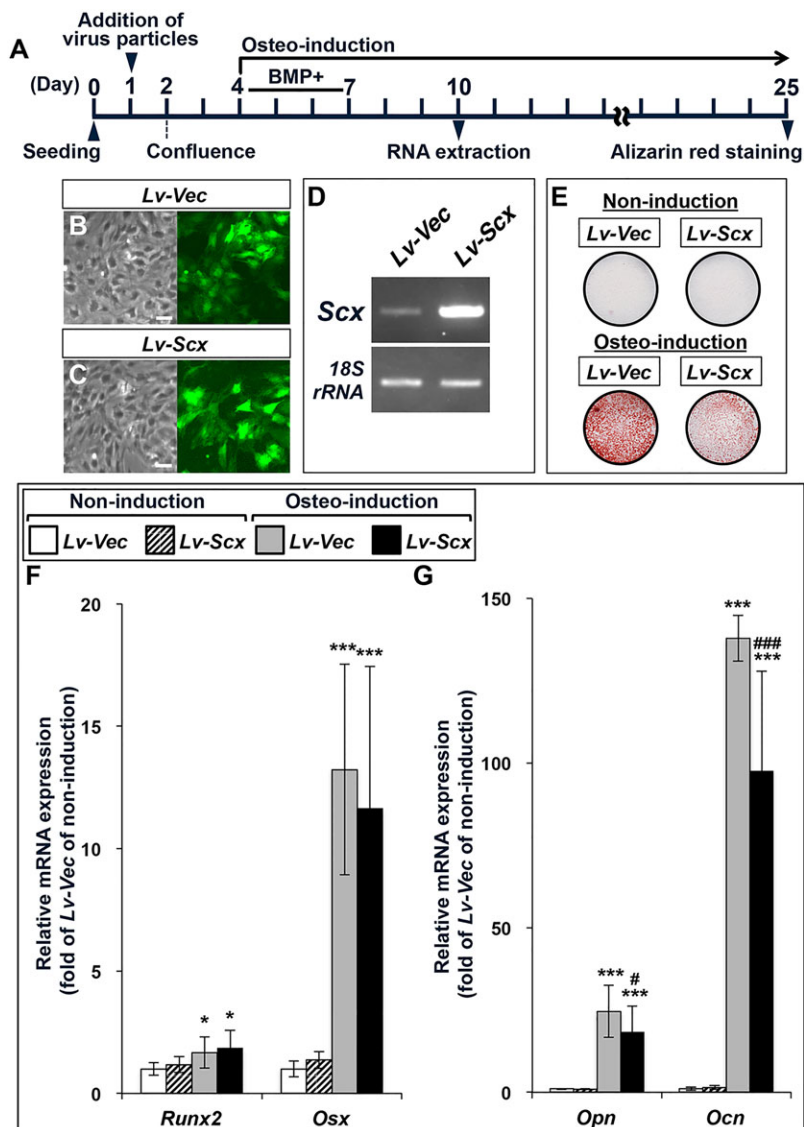
DEVELOPMENT

Fig. 6. Inhibitory action of *Scx* on mineralization of PDL cells cultured under osteogenic conditions. (A) PDL cells were seeded at a density of 2×10^4 or 4×10^4 cells/well in a 24-well or 12-well plate, respectively. At 24 h after inoculation, the cells were infected with *Lv-Vec* or *Lv-Scx*. The cells were grown in α-MEM containing 10% FBS and reached confluence on day 2. For osteogenic induction (osteo-induction), the cultures on day 4 were switched to an induction medium containing rhBMP6, maintained for 3 days and further maintained in induction medium without rhBMP6 for another 3 or 18 days. Non-inducing cultures were maintained in α-MEM containing 10% FBS throughout the culture period. (B,C) Morphology of PDL cells cultured in α-MEM containing 10% FBS at day 10. Infected cells expressing GFP were detected in 75% or 78% of the cells infected with *Lv-Vec* or *Lv-Scx*, respectively. (D) RT-PCR analysis for *Scx* or *18S rRNA*. The primer set for *Scx* was designed to detect endogenous and lentiviral expression. *Scx* and *18S rRNA* were amplified by 30 and 25 cycles, respectively. (E) PDL cells cultured under the non-induction or osteo-induction conditions were stained with Alizarin Red on day 25. (F,G) Total RNA was extracted from PDL cells on day 10. Relative expression levels of *Runx2*, *Osx*, *Opn* and *Ocn* were examined by RT-qPCR. The data represent the average of three independent experiments. The relative expression of each gene is normalized to *Lv-Vec* of Non-induction and reported as mean±s.d. *$P<0.05$ versus *Lv-Vec* of non-induction, ***$P<0.001$ versus *Lv-Vec* of non-induction, #$P<0.05$ versus *Lv-Vec* of osteo-induction, ###$P<0.001$ versus *Lv-Vec* of osteo-induction. Scale bars: 100 μm.

that Mgp, asporin, msh homeobox 2 (Msx2) and twist-related protein 1 (Twist1) act as inhibitors of the mineralization of the PDL (Hashimoto et al., 2001; Kaipatur et al., 2008; Komaki et al., 2007; Murshed et al., 2004; Yamada et al., 2007; Yoshizawa et al., 2004). *Scx* is also a member of the twist subfamily of basic helix-loop-helix transcription factors (Atchley and Fitch, 1997). The inhibitory action of Pstn on mineralization was reported using an odontoblastic cell line (Ma et al., 2011). We found that not only Scx but also Pstn were significantly upregulated on the tensile force-loaded site of the PDL. Under non-inducing conditions, *Mgp* and *Pstn* were significantly upregulated by *Scx* overexpression. *Pstn* was significantly downregulated in PDL cells by osteoinduction, whereas its expression was recovered by *Scx* overexpression. These results suggest that Scx also participates in keeping the PDL unmineralized in concert with previously reported molecules.

Scx[+]/Sox9^{+} progenitors contribute to the establishment of the junction between cartilage and tendon/ligament (Blitz et al., 2013; Sugimoto et al., 2013a). Interestingly, the PDL and alveolar bone are also derived from *Scx[+]/Sox9^{+}* progenitors (unpublished data). In this study, we demonstrated that the Scx[+]/Osx[−], Scx[+]/Osx[+] and Scx[−]/Osx[+] PDL cell populations participate coordinately in

remodeling and maintaining the junction between the cementum of the tooth and the alveolar bone. As reported previously, αSMA[+] progenitor/stem cells in the perivascular regions of the PDL can differentiate into osteoblasts, cementoblasts and fibroblasts (Roguljic et al., 2013; San Miguel et al., 2010). However, expression of αSMA in the PDL did not overlap with Scx expression, suggesting that fibroblastic Scx^{+} PDL cells respond to the mechanical stress to quickly participate in PDL remodeling. The increase in the number of the pSmad1/5^{+} PDL cells and Osx^{+} PDL cells on the tension side suggests that PDL cells become more osteogenic through the activation of BMP signaling upon tensile force loading. Osx-driven osteogenesis in the PDL is counteracted by the increased expression of Scx, which facilitates ligamentogenic fibroblast maturation and inhibits osteogenic mineralization. The *Scx[high]/Osx[+]* cell population appears on the tension side of the PDL that does not calcify, whereas the *Scx[−]/Osx[+]* cells and osteogenic PDL cells with weak Scx expression reside close to the alveolar bone. The balance of Scx and Osx activities can be a determinant of the decision whether PDL cells follow either the fibroblastic or osteogenic differentiation pathway. Further studies are now underway to explore how the position-specific upregulation of Scx is regulated in the tensile force-responsive PDL.
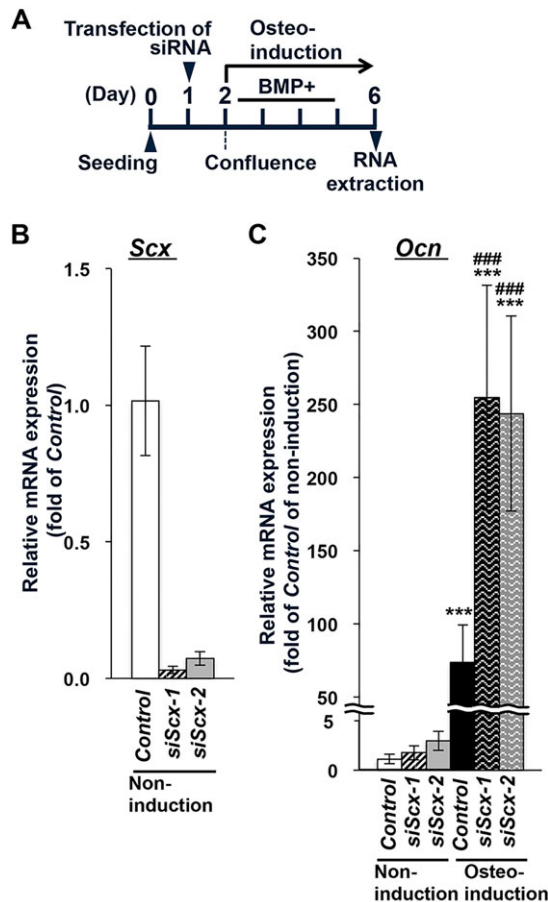
Fig. 7. Upregulation of *Ocn* by *Scx* knockdown in PDL cells under osteogenic conditions. (A) PDL cells were seeded at a density of 2×10^4 cells/well in a 24-well plate. At 24 h after inoculation, the cells were transfected with *non-targeting* siRNA (control) or *Scx* siRNAs (*siScx-1* or *siScx-2*) by lipofection. The cells were grown in α-MEM containing 10% FBS and reached confluence on day 2. For osteogenic induction (osteo-induction), the cultures on day 2 were switched to an induction medium containing rhBMP6, maintained for 3 days and further maintained in induction medium without rhBMP6 up to day 6. Non-inducing cultures were maintained in α-MEM containing 10% FBS. (B,C) Total RNA was extracted from PDL cells on day 6 and the expression levels of *Scx* (B) or *Ocn* (C) were examined by RT-qPCR. The data represent the average of three independent experiments. The relative expression of each gene is normalized to *control* of non-induction and reported as mean±s.d. ***$P<0.001$ versus *control* of non-induction, ###$P<0.001$ versus *control* of osteo-induction.

MATERIALS AND METHODS

Animals

C57BL/6 mice and Wistar rats were purchased from Shimizu Laboratory Supplies (Kyoto, Japan). The generation and establishment of *ScxGFP* transgenic strains have been reported previously (Sugimoto et al., 2013b). Scx expression was monitored by GFP expression. All animal experimental procedures used in this study were approved by the Animal Care Committee of the Institute for Frontier Medical Sciences, Kyoto University, Japan, and conformed to institutional guidelines for the study of vertebrates.

Experimental tooth movement

Nine-week-old *Scx-GFP* Tg male mice were subjected to experimental tooth movement. These mice were anesthetized by intraperitoneal injection of sodium pentobarbital (30 mg/kg) (Kyoritsu Seiyaku, Tokyo, Japan). Experimental tooth movement was achieved by the interproximal insertion of a piece of orthodontic elastic band between the upper first and second molars on the left side, according to the method
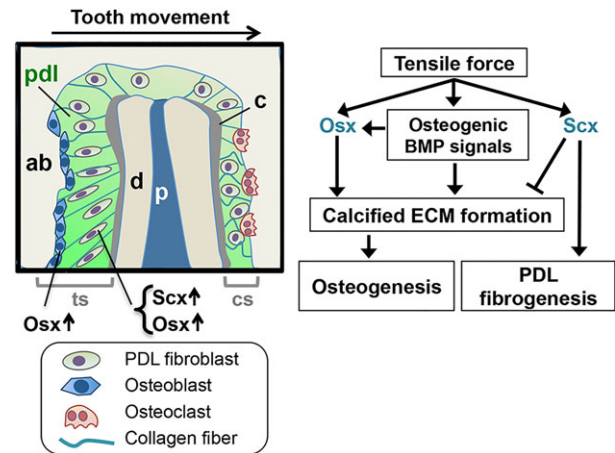

Fig. 8. Model for tensile force-responsive remodeling of the periodontal tissues during the tooth movement. Tensile force upregulates directly or indirectly Scx and Osx in the PDL. Osteogenic BMP signals induced by tensile force also upregulate Osx and facilitate osteogenesis to form calcified ECM at the PDL-bone interface. Scx acts as a negative regulator of PDL mineralization. ab, alveolar bone; c, cementum; cs, compression side; d, dentin; pdl, periodontal ligament; ts, tension side.

described by Waldo and Rothblatt (1954). The contralateral right side was used as a control. At 48 h after insertion, a maxillary impression was taken using silicon impression material under anesthesia. The impressions were filled with dental stone, and the distance between the first and second molars was measured using a dial tension gauge (Mitutoyo, Kanagawa, Japan).

Histological staining

For hematoxylin and eosin (H&E) staining, sections were stained with Gill's hematoxylin (Vector Laboratories) and 0.25% eosin (Sigma). To detect ALP activity, non-decalcified frozen sections were covered with a 2% Nitro-Blue tetrazolium chloride/5-bromo-4-chloro-3′-indolyphosphatase p-toluidine salt stock solution (Roche) diluted in ALP buffer at pH 9.5 (100 mM Tris-HCl, 100 mM NaCl, 50 mM $MgCl_2$) and then incubated for 5 min at 37°C in the dark. PDL cells were fixed with 95% methanol for 20 min and stained with 1% Alizarin Red S (Wako) at pH 6.4 for 16 h.

Immunostaining

Anesthetized mice were perfused with 4% paraformaldehyde in phosphate-buffered saline (PFA/PBS) containing 20% sucrose, and their upper jaws or legs were dissected. The specimens were fixed in 4% PFA/PBS containing 20% sucrose for 3 h, embedded in SCEM (Section-Lab), and frozen in *n*-hexane cooled with dry ice. Undecalcified frozen sections at a thickness of 4 μm were obtained according to Kawamoto's film method using tungsten carbide blades, either TC-65 (Leica Microsystems) or SL-T35 (Section-Lab), and adhesive films (Section-Lab) (Kawamoto, 2003). After washing with ethanol and PBS, the sections were fixed in 4% PFA/PBS for 5 min and decalcified with 0.25 M ethylenediaminetetraacetic acid (EDTA)/PBS for 1 h. Sections for the detection of Osx, αSMA or pSmad1/5 were boiled in 10 mM sodium acetate at pH 6 for 10 min. After blocking with 3.2% skim milk/PBS, the sections were incubated with primary antibodies for 16 h, washed and then incubated with appropriate secondary antibodies conjugated with Alexa Fluor 488 or 594 (Life Technologies). Nuclei were counterstained with 4′,6-diamidino-2-phenylindole (DAPI) (Sigma). The primary antibodies used were anti-GFP (rat IgG2a) (Nakarai Tesque, 04404-84; 1:1000), anti-GFP (rabbit IgG) (MBL, 598; 1:1000), anti-CD31 (BD, 553370; 1:1000), anti-osteocalcin (anti-Ocn) (Takara Bio, M173; 1:800), anti-Osx (Abcam, ab22552; 1:800), anti-periostin (anti-Pstn) (BioVendor, RD181045050; 1:800), anti-αSMA (Abcam, ab5694; 1:500) and anti-pSmad1/5 (Cell Signaling, #9516S; 1:100). The images were captured under a Leica DMRXA microscope equipped with a Leica DC500 camera (Leica

Table 1. Primers for RT-qPCR

Gene		Sequence (5'-3')
Ocn	Forward	GGTGCAGACCTAGCAGACACCA
	Reverse	AGGTAGCGCCGGAGTCTATTCA
Opn	Forward	AGACCATGCAGAGAGCGAG
	Reverse	ACGTCTGCTTGTGTGCTGG
Osx	Forward	CACCCATTGCCAGTAATCTTCGT
	Reverse	GGACTGGAGCCATAGTGAGCTTCT
Runx2	Forward	CACAGGGTGACTCCCGTTACAA
	Reverse	TGTGACCCAGTGCAAATGAAGA
Scx	Forward	AGCCCAAACAGATCTGCACCTT
	Reverse	CTTCCACCTTCACTAGTGGCATCA
18S rRNA	Forward	AAGTTTCAGCACATCCTGCGAGTA
	Reverse	TTGGTGAGGTCAATGTCTGCTTTC

Microsystems). After acquisition of the fluorescent images, HE staining was performed on the same sections.

Quantification of Scx^{high} cells

Images of the specimens subjected to experimental tooth movement were acquired under the same conditions using a GFP filter with a 1 s exposure. To determine high expression levels using the brightness of a color given the RGB values, areas with high brightness were selected automatically in the green channel image using Adobe Photoshop CS3 (Adobe Systems). Scx^{high} cells were defined as cells with a brightness >2.5-fold higher than the background level (dentin area) in green channel images. Nuclei labeled with DAPI were counted.

Cell culture

PDL cells were isolated from 4-week-old male Wistar rats. The maxillary and mandibular first, second and third molars were extracted and washed with PBS. The PDL attached to the middle of the root surface was scraped off, placed onto 35-mm cell culture dishes (BD) and maintained in MF-start (TOYOBO). At confluence, the cells outgrown from the PDL were passaged twice and grown in minimum essential medium Eagle alpha modification (α-MEM) supplemented with 10% fetal bovine serum (FBS). Cells were maintained in a humidified atmosphere of 5% CO_2 in air.

Osteogenic induction and alizarin red staining

For osteoinduction, PDL cells were maintained in α-MEM supplemented with 10% FBS, 1 μM dexamethasone, 10 mM β-glycerophosphate, 50 μg/ml ascorbic acid and 200 ng/ml of recombinant human (rh) BMP6 (differentiation medium) for 3 days, and then cultured in differentiation medium without rhBMP6 for another 21 days, as reported previously (Hakki et al., 2014; Yoshizawa et al., 2004).

Lentiviral overexpression

Lentiviral particles were produced using HIV-based lentiviral vector constructs purchased from SBI. The full coding DNA fragment of mouse Scx was inserted into the pCDH-CMV-MCS-EF1-GreenPuro vector (SBI). The lentiviral particles were concentrated with PEG-it virus precipitation solution (SBI), and the multiplicity of infection (MOI) in NIH3T3 cells was titrated using a Global Ultra Rapid Lentiviral Titer Kit (SBI). For PDL cells, 1.0 MOI of the lentiviral particles were used.

Scx knockdown by RNA interference

Small interfering RNA (siRNA) oligonucleotide duplexes were purchased from GE Healthcare Life Sciences. Scx was knocked down using siScx-1 (catalog number J-113656-09) and siScx-2 (catalog number J-113656-10) included in the ON-TARGET plus rat Scx siRNA-Set of 4 (catalog number LQ-113656-00-002). For the control experiment, siGENOME non-targeting siRNA Pool number 1 (catalog number D-001206-13-05) was used. Transfection of siRNA into PDL cells was performed with DharmaFECT 1 transfection reagent (GE Healthcare Life Sciences) according to the manufacturer's instructions.

Reverse transcriptase-polymerase chain reaction (RT-PCR) and quantitative RT-PCR (RT-qPCR) analysis

Total RNA was extracted from PDL cells using an RNeasy Plus Mini Kit (QIAGEN). Two hundred nanograms of total RNA were used to synthesize complementary DNA (cDNA) with a PrimeScript RT reagent Kit (Takara Bio). RT-PCR was performed with Takara Ex Taq (Takara Bio) and specific primers for Scx (forward, 5'-GCAGCGGCACACAGCGAAT-3'; reverse, 5'-AGGCGCAGCGTCTCAATCT-3'). RT-qPCR was performed using SYBR Premix Ex Taq II (Takara Bio) on a StepOne instrument (Life Technologies). Relative mRNA expression was normalized to 18S rRNA and calculated using the $2^{-\Delta\Delta CT}$ method. Specific primers for RT-qPCR are listed in Table 1.

Statistical analysis

P-values were calculated by t-test or one-way analysis of variance using the SPSS software package (SPSS 21.0). Data were considered statistically significant for a P-value <0.05.

References

Atchley, W. R. and Fitch, W. M. (1997). A natural classification of the basic helix-loop-helix class of transcription factors. *Proc. Natl. Acad. Sci. USA* **94**, 5172-5176.

Beertsen, W., McCulloch, C. A. G. and Sodek, J. (1997). The periodontal ligament: a unique, multifunctional connective tissue. *Periodontology 2000* **13**, 20-40.

Benjamin, M. and Ralphs, J. R. (2000). The cell and developmental biology of tendons and ligaments. *Int. Rev. Cytol.* **196**, 85-130.

Blitz, E., Sharir, A., Akiyama, H. and Zelzer, E. (2013). Tendon-bone attachment unit is formed modularly by a distinct pool of Scx- and Sox9-positive progenitors. *Development* **140**, 2680-2690.

Brent, A. E., Schweitzer, R. and Tabin, C. J. (2003). A somitic compartment of tendon progenitors. *Cell* **113**, 235-248.

Cao, Z., Zhang, H., Zhou, X., Han, X., Ren, Y., Gao, T., Xiao, Y., de Crombrugghe, B., Somerman, M. J. and Feng, J. Q. (2012). Genetic evidence for the vital function of Osterix in cementogenesis. *J. Bone Miner. Res.* **27**, 1080-1092.

Cserjesi, P., Brown, D., Ligon, K. L., Lyons, G. E., Copeland, N. G., Gilbert, D. J., Jenkins, N. A. and Olson, E. N. (1995). Scleraxis: a basic helix-loop-helix protein that prefigures skeletal formation during mouse embryogenesis. *Development* **121**, 1099-1110.

Docheva, D., Hunziker, E. B., Fassler, R. and Brandau, O. (2005). Tenomodulin is necessary for tenocyte proliferation and tendon maturation. *Mol. Cell. Biol.* **25**, 699-705.

Hakki, S. S., Bozkurt, B., Hakki, E. E., Kayis, S. A., Turac, G., Yilmaz, I. and Karaoz, E. (2014). Bone morphogenetic protein-2, -6, and -7 differently regulate osteogenic differentiation of human periodontal ligament stem cells. *J. Biomed. Mater. Res. B Appl. Biomater.* **102**, 119-130.

Hashimoto, F., Kobayashi, Y., Kobayashi, E. T., Sakai, E., Kobayashi, K., Shibata, M., Kato, Y. and Sakai, H. (2001). Expression and localization of MGP in rat tooth cementum. *Arch. Oral Biol.* **46**, 585-592.

Henneman, S., Von den Hoff, J. W. and Maltha, J. C. (2008). Mechanobiology of tooth movement. *Eur. J. Orthodont.* **30**, 299-306.

Inamasu, J., Guiot, B. H. and Sachs, D. C. (2006). Ossification of the posterior longitudinal ligament: an update on its biology, epidemiology, and natural history. *Neurosurgery* **58**, 1027–1039; discussion 1027-1039.

DEVELOPMENT

Kaipatur, N. R., Murshed, M. and McKee, M. D. (2008). Matrix Gla protein inhibition of tooth mineralization. *J. Dent. Res.* **87**, 839-844.

Kawamoto, T. (2003). Use of a new adhesive film for the preparation of multi-purpose fresh-frozen sections from hard tissues, whole-animals, insects and plants. *Arch. Histol. Cytol.* **66**, 123-143.

Kimura, N., Shukunami, C., Hakuno, D., Yoshioka, M., Miura, S., Docheva, D., Kimura, T., Okada, Y., Matsumura, G., Shin'oka, T. et al. (2008). Local tenomodulin absence, angiogenesis, and matrix metalloproteinase activation are associated with the rupture of the chordae tendineae cordis. *Circulation* **118**, 1737-1747.

Komaki, M., Karakida, T., Abe, M., Oida, S., Mimori, K., Iwasaki, K., Noguchi, K., Oda, S. and Ishikawa, I. (2007). Twist negatively regulates osteoblastic differentiation in human periodontal ligament cells. *J. Cell. Biochem.* **100**, 303-314.

Komiyama, Y., Ohba, S., Shimohata, N., Nakajima, K., Hojo, H., Yano, F., Takato, T., Docheva, D., Shukunami, C., Hiraki, Y. et al. (2013). Tenomodulin expression in the periodontal ligament enhances cellular adhesion. *PLoS ONE* **8**, e60203.

Komori, T., Yagi, H., Nomura, S., Yamaguchi, A., Sasaki, K., Deguchi, K., Shimizu, Y., Bronson, R. T., Gao, Y.-H., Inada, M. et al. (1997). Targeted disruption of Cbfa1 results in a complete lack of bone formation owing to maturational arrest of osteoblasts. *Cell* **89**, 755-764.

Ma, D., Zhang, R., Sun, Y., Rios, H. F., Haruyama, N., Han, X., Kulkarni, A. B., Qin, C. and Feng, J. Q. (2011). A novel role of periostin in postnatal tooth formation and mineralization. *J. Biol. Chem.* **286**, 4302-4309.

Mabuchi, R., Matsuzaka, K. and Shimono, M. (2002). Cell proliferation and cell death in periodontal ligaments during orthodontic tooth movement. *J. Periodont. Res.* **37**, 118-124.

Maeda, T., Sakabe, T., Sunaga, A., Sakai, K., Rivera, A. L., Keene, D. R., Sasaki, T., Stavnezer, E., Iannotti, J., Schweitzer, R. et al. (2011). Conversion of mechanical force into TGF-beta-mediated biochemical signals. *Curr. Biol.* **21**, 933-941.

Maes, C., Kobayashi, T., Selig, M. K., Torrekens, S., Roth, S. I., Mackem, S., Carmeliet, G. and Kronenberg, H. M. (2010). Osteoblast precursors, but not mature osteoblasts, move into developing and fractured bones along with invading blood vessels. *Dev. Cell* **19**, 329-344.

Murchison, N. D., Price, B. A., Conner, D. A., Keene, D. R., Olson, E. N., Tabin, C. J. and Schweitzer, R. (2007). Regulation of tendon differentiation by scleraxis distinguishes force-transmitting tendons from muscle-anchoring tendons. *Development* **134**, 2697-2708.

Murshed, M., Schinke, T., McKee, M. D. and Karsenty, G. (2004). Extracellular matrix mineralization is regulated locally; different roles of two gla-containing proteins. *J. Cell Biol.* **165**, 625-630.

Nakashima, K., Zhou, X., Kunkel, G., Zhang, Z., Deng, J. M., Behringer, R. R. and de Crombrugghe, B. (2002). The novel zinc finger-containing transcription factor osterix is required for osteoblast differentiation and bone formation. *Cell* **108**, 17-29.

Oshima, Y., Sato, K., Tashiro, F., Miyazaki, J.-i., Nishida, K., Hiraki, Y., Tano, Y. and Shukunami, C. (2004). Anti-angiogenic action of the C-terminal domain of tenomodulin that shares homology with chondromodulin-I. *J. Cell Sci.* **117**, 2731-2744.

Pavlin, D. and Gluhak-Heinrich, J. (2001). Effect of mechanical loading on periodontal cells. *Crit. Rev. Oral Biol. Med.* **12**, 414-424.

Roguljic, H., Matthews, B. G., Yang, W., Cvija, H., Mina, M. and Kalajzic, I. (2013). In vivo identification of periodontal progenitor cells. *J. Dent. Res.* **92**, 709-715.

San Miguel, S. M., Fatahi, M. R., Li, H., Igwe, J. C., Aguila, H. L. and Kalajzic, I. (2010). Defining a visual marker of osteoprogenitor cells within the periodontium. *J. Periodont. Res.* **45**, 60-70.

Schweitzer, R., Chyung, J. H., Murtaugh, L. C., Brent, A. E., Rosen, V., Olson, E. N., Lassar, A. and Tabin, C. J. (2001). Analysis of the tendon cell fate using Scleraxis, a specific marker for tendons and ligaments. *Development* **128**, 3855-3866.

Scott, A., Danielson, P., Abraham, T., Fong, G., Sampaio, A. V. and Underhill, T. M. (2011). Mechanical force modulates scleraxis expression in bioartificial tendons. *J. Musculoskelet. Neuronal Interact.* **11**, 124-132.

Seo, B.-M., Miura, M., Gronthos, S., Bartold, P. M., Batouli, S., Brahim, J., Young, M., Robey, P. G., Wang, C. Y. and Shi, S. (2004). Investigation of multipotent postnatal stem cells from human periodontal ligament. *Lancet* **364**, 149-155.

Shukunami, C., Takimoto, A., Oro, M. and Hiraki, Y. (2006). Scleraxis positively regulates the expression of tenomodulin, a differentiation marker of tenocytes. *Dev. Biol.* **298**, 234-247.

Shukunami, C., Takimoto, A., Miura, S., Nishizaki, Y. and Hiraki, Y. (2008). Chondromodulin-I and tenomodulin are differentially expressed in the avascular mesenchyme during mouse and chick development. *Cell Tissue Res.* **332**, 111-122.

Sugimoto, Y., Takimoto, A., Akiyama, H., Kist, R., Scherer, G., Nakamura, T., Hiraki, Y. and Shukunami, C. (2013a). Scx+/Sox9+ progenitors contribute to the establishment of the junction between cartilage and tendon/ligament. *Development* **140**, 2280-2288.

Sugimoto, Y., Takimoto, A., Hiraki, Y. and Shukunami, C. (2013b). Generation and characterization of ScxCre transgenic mice. *Genesis* **51**, 275-283.

Takano-Yamamoto, T., Takemura, T., Kitamura, Y. and Nomura, S. (1994). Site-specific expression of mRNAs for osteonectin, osteocalcin, and osteopontin revealed by in situ hybridization in rat periodontal ligament during physiological tooth movement. *J. Histochem. Cytochem.* **42**, 885-896.

Terai, K., Takano-Yamamoto, T., Ohba, Y., Hiura, K., Sugimoto, M., Sato, M., Kawahata, H., Inaguma, N., Kitamura, Y. and Nomura, S. (1999). Role of osteopontin in bone remodeling caused by mechanical stress. *J. Bone Miner. Res.* **14**, 839-849.

Waldo, C. M. and Rothblatt, J. M. (1954). Histologic response to tooth movement in the laboratory rat: procedure and preliminary observations. *J. Dent. Res.* **33**, 481-486.

Yamada, S., Tomoeda, M., Ozawa, Y., Yoneda, S., Terashima, Y., Ikezawa, K., Ikegawa, S., Saito, M., Toyosawa, S. and Murakami, S. (2007). PLAP-1/asporin, a novel negative regulator of periodontal ligament mineralization. *J. Biol. Chem.* **282**, 23070-23080.

Yamashita, Y., Sato, M. and Noguchi, T. (1987). Alkaline phosphatase in the periodontal ligament of the rabbit and macaque monkey. *Arch. Oral Biol.* **32**, 677-678.

Yoshizawa, T., Takizawa, F., Iizawa, F., Ishibashi, O., Kawashima, H., Matsuda, A., Endo, N. and Kawashima, H. (2004). Homeobox protein MSX2 acts as a molecular defense mechanism for preventing ossification in ligament fibroblasts. *Mol. Cell. Biol.* **24**, 3460-3472.

DEVELOPMENT